Since January 2020 Elsevier has created a COVID-19 resource centre with free information in English and Mandarin on the novel coronavirus COVID-19. The COVID-19 resource centre is hosted on Elsevier Connect, the company's public news and information website.

Colloids and Surfaces B: Biointerfaces 214 (2022) 112465

Contents lists available at ScienceDirect

Colloids and Surfaces B: Biointerfaces

journal homepage: www.elsevier.com/locate/colsurfb

Interactions between glucosides of the tip of the S1 subunit of SARS-CoV-2 spike protein and dry and wet surfaces of CuO and Cu—A model for the surfaces of coinage metals

Cláudio M. Lousada

Department of Materials Science and Engineering, KTH Royal Institute of Technology, SE-100 44 Stockholm, Sweden

ARTICLE INFO

Keywords:
Quantum mechanical modeling
SARS-CoV-2
Spike protein
Interactions with inorganic surfaces
DFT

ABSTRACT

Despite their importance there is little knowledge at the atomic scale on the interactions between fragments of SARS-CoV-2 and inorganic materials. Such knowledge is important to understand the survival of the virus at surfaces and for the development of antiviral materials. Here is reported a study of the interactions between glucoside monomers of the tip of the S1 subunit of SARS-CoV-2 spike protein with dry and wet surfaces of CuO and Cu, performed with dispersion corrected density functional theory—DFT. The three glucoside monomers that constitute the tip of S1: 6VSB, 6VXX and 6X6P, were adsorbed onto dry and wet CuO(111) and Cu(110) with different orientations and surface alignments.

There are large differences—of up to 1.3 eV—in binding energies between these monomers and the surfaces. These differences depend on: the type of surface; if the surface is wet or dry; if the glucosidic O-atom points towards or away from the surfaces; and to a smaller extent on the surface alignment of the monomers. All monomers bind strongly to the surfaces via molecular adsorption that does not involve bond breaking in the monomers at this stage. 6VSB has the larger adsorption energies—that reach 2.2 eV—due to its larger dipole moment. Both materials bind the monomers more strongly when their surfaces are dry. At Cu(110) the bonds are on average 1 eV stronger when the surface is dry when compared to wet. The difference between dry and wet CuO(111) is smaller, in the order of 0.2 eV. Overall, it is here shown that the stability of the monomers of the tip of the spike protein of the virus is very different at different surfaces. For a given surface the larger binding energies in dry conditions could explain the differences in the surface stability of the spike protein depending on the presence of moisture.

1. Introduction

COVID-19 the disease caused by the coronavirus SARS-CoV-2 is an emergency that has caused enormous damages to mankind. Roughly one year after the first reported global cases, a great deal of knowledge about the virus responsible for the disease has been gathered. However, to this date, there are still many unknowns regarding the survival of the virus outside the human body, especially at the inorganic surfaces that constitute the world around us. Some reports claim that this virus, as previously found for other coronaviruses [1], has the ability to survive on surfaces for hours or even days [2] while other reports claim that the viral RNA found on surfaces are only dispersed fragments and thus not able to infect living organisms because these fragments are part of a virus that has been damaged and as such inactivated [3]. Based on the current knowledge on how different surfaces have very different ability to drive chemical processes, such observations will certainly, to a large extent, depend on the type of surface and its environment [4–10].

The rush for gaining knowledge on the agent that causes the disease has led to an array of important publications with details on the structure of the virus down to the range of the 10 Å [11]. While a lot of work has—fortunately—been done in this area, up to date there are only few accounts of studies that have focused on mechanistic details of the interactions of the virus with inorganic surfaces [12]. It is important to understand these interactions because such surfaces have the potential to act as virus reservoirs [1,2]. Knowing the atomic scale mechanisms behind these interactions is essential to develop better understanding of the physical-chemical properties of virus, to understand the performance of different modeling methods and can guide the design of effective antiviral surfaces and coatings.

Because the interactions of most organic matter with inorganic

E-mail address: cmlp@kth.se.

https://doi.org/10.1016/j.colsurfb.2022.112465
Received 11 October 2021; Received in revised form 14 March 2022; Accepted 15 March 2022
Available online 23 March 2022

surfaces are largely controlled by anisotropic dispersion forces [13,14], the challenge of understanding the details of the interactions between the virus with these surfaces is enormous. This is a task not easily at reach of current experimental methods, and the computational methods purely based on classical force-fields fail to account properly for those forces. This is because of the lack of accurate parameters for such a heterogeneous system—consisting of the inorganic components: metals, oxides, etc; in contact with organic matter, the virus. The solution to this problem is then to model the system with modeling tools based on quantum mechanics. But because employing high level quantum mechanical computations to the whole virus—or even to large pieces—is not at reach of our current computational tools, the challenge here is to find suitable models and computational tools that can be used to model important parts of the system virus-surfaces with good accuracy.

Studies on the virus structure have shown that the spike proteins located at the surface of the virus are important mediators of the interactions between the virus and its environment [15]. The tip of the spike proteins of the intact virus is composed of the so-called subunit S1 [11]. This subunit is in turn connected to the subunit S2. S1 acts as a sensor for the medium and can transmit that information further to S2 via a series of structural and chemical changes that occur at the interface between S1 and S2 [11]. Among other things this process mediates the entry of the virus into cells [16,17] and the S1 subunit is the target of an array of vaccine concepts [18–20]. At the tip of S1 there are three monomers of glucosides [11,15]. The detailed structures of those monomers have been published and have the PDB identities 6VSB [21], 6VXX [22], and 6X6P [23], Because these monomers are the contact points between the virus and the environment, understanding their interactions with inorganic surfaces can give important mechanistic information on how such surfaces may affect the virus.

Coinage metals, the elements from group 11 in the periodic table, are important materials in our daily life, for which copper is often used as a model due to their similarities [24–27]. The mechanisms of the interactions between the SARS-CoV-2 virus and these materials are not known, but it is well known that the surface of metallic copper in ambient conditions is terminated by a native oxide layer with considerable thickness which affects the chemical-physical properties of the material [28]. The outer oxide is tenorite, CuO, can have a thickness of up to 0.5 nm and its most stable surface, the (111) [29], adsorbs water from the environment in a wide range of temperatures and partial pressures of water [30,31]. The first monolayer (ML) of adsorbed water consists of a mixed structure composed of both dissociatively adsorbed water and molecularly adsorbed water. In these adsorption modes, water binds to the surface with considerable adsorption energies (ΔE_{ads}) of ≈ -0.70 eV/H_2O to ≈ -0.5 eV/H_2O respectively [30,31]. The dissociative adsorption of H_2O at this surface proceeds via the typical mechanism where upon dissociation of H_2O, the HO bind to bare Cu-atoms and the H bind to bare O-atoms forming in both cases surface sites terminated by HO groups. The large ΔE_{ads} for H_2O imply that this mixed layer of H_2O and HO is stable at room temperature [30]. Because of this, when modeling the interactions between copper with molecules in ambient air, it is important to account for the fact that in moisty air, at the atomic scale, it is the hydrated-hydroxylated surface of CuO which is responsible for the interactions with adsorbates.

The mechanisms and strength of the interactions between organic molecules and surfaces can be highly specific depending on the presence of surface bound water as described above, but also on properties intrinsic to the respective organic molecules [4–6]. This is because of the effect that the electronic structure of adsorbates has in determining their interactions with surfaces. The presence of certain functional groups and of certain types of intramolecular bonds—single, double, triple bonds, non-bonded electrons, and resonance structures among others—will largely affect the adsorption mechanisms and energies. Such knowledge is difficult to obtain experimentally, but recently, due to the increased computational power, a very valuable tool at our disposal for such investigations is quantum mechanical modeling together with periodic models of the surfaces [32–36]. For the case of the interactions between the surfaces here studied with glucosides—and other sugars in general—there is no detailed mechanistic nor energetic data, especially with the level of detail that can be obtained with quantum mechanical modeling methods.

In this work the interactions between the glucoside monomers 6VSB, 6VXX and 6X6P and the most stable surfaces of CuO and Cu were investigated with dispersion corrected density functional theory (DFT) and surface models with periodic boundary conditions. The models here employed have been conceived so that to a large extent they mimic Cu and its native oxide exposed to dry and moisty air in ambient conditions. The differences in binding energies between the different monomers and the surfaces are very large, up to 1.3 eV and depend largely on the material, on the presence of water at a given surface and on the orientation of the monomer.

2. Computational details

The electronic structure calculation methods here employed have been previously extensively tested and benchmarked in varied studies of adsorption on pure and oxidized Cu surfaces as well as hydroxylated Cu surfaces [37–39]. DFT calculations were performed with the Vienna ab initio simulation package [40] (VASP 5.4.4) employing the exchange-correlation functional by Perdew-Burke-Ernzerhof, PBE (Refs [41,42].) with pseudopotentials of the projector augmented wave [43, 44] (PAW) type which are coherent with the ultrasoft type. The van der Waals interactions which are important for the correct description of the structure of hydrogen bonded structures [45–47] were described with the zero damping D3 correction [48] by Grimme as implemented in VASP. The PBE functional with corrections of the D type has shown good performance for modeling complex hydrogen bonded structures and for the description of adsorption and desorption in structures dominated by H-bonds [45,47]. For the geometry optimizations and single point energy calculations, a plane wave cutoff energy of 560 eV and a k-point mesh of (2 ×2 ×1) in the Monkhorst-Pack sampling scheme [49] were used together with Gaussian smearing with a width of 0.05 eV.

Stoichiometric monoclinic CuO(111) [50], and fcc Cu(110), were simulated with periodically repeating slabs in supercells with surface symmetries $p(3\times2)$ and $p(3\times3)$ respectively, and vacuum thicknesses of 15 Å and 25 Å respectively. For CuO(111), the slab consisted of 128 atoms with a thickness of 2 stoichiometric unit cells of CuO. For the geometry optimizations the bottom layer was constrained, and the remaining atoms were relaxed. The slab of Cu(110) consisted of 108 Cu-atoms disposed in 3 layers where the bottom layer was constrained and the remaining atoms were relaxed. To model the wet surfaces, both surfaces were hydrated-hydroxylated according to the literature knowledge for when these materials are exposed to a water containing environment, such as moisty air [30,37]. The adsorption energies (ΔE_{ads}) reported herein have been determined as

$$\Delta E_{ads} = E_{product} - \sum E_{reactants} \quad (1)$$

where $E_{product}$ represents the electronic energy of the adsorbate bound to the slab and $E_{reactants}$, represents the electronic energy of the bare slab and that of the adsorbate in gas-phase. A more negative value for ΔE_{ads} implies stronger adsorption.

The glucoside monomers of the tip of the subunit S1 of the SARS-coV-2 spike protein: 6VSB [21], 6VXX [22], and 6X6P [23], were retrieved from PDB. These monomers consist of isomers of 2-acetamido-2-deoxy-beta-D-glucopyranose. The retrieved conformations are the AA for every monomer and have been chosen in order to have monomers both in cis and in trans conformations. The monomers have been disposed at the surfaces one by one with their main axis parallel to each surface plane vector and in conformations in between. After this, a geometry optimization was performed where all atoms of the monomers and all atoms of the surface slabs except the bottom layer were allowed to relax. Only the most stable conformations obtained are here presented and discussed.

Solvation effects have been simulated with VASPsol which adds an implicit solvation model to VASP [51,52] and where water with a dielectric constant of 78.3 at 25 °C has been used. Test calculations for selected cases revealed that the solvation contribution to the adsorption energies varied from 0.08 eV for CuO(111) to 0.21 eV for Cu(110). The decrease of the adsorption energies is very small for all cases investigated due to the large magnitude of the adsorption energies in comparison with the contribution from the solvation effects. For molecular adsorption as studied here, the solvation energies of the fragments are close to constant during the reaction, as it has been previously observed for H_2O [37], The exception to this is the solvation at the interface between the fragments and the surfaces which has been here explicitly considered with wet surface models as detailed below. Because the interface solvation is the most relevant for the interactions between the viruses and surfaces [53] and given that the contribution of the solvation is very small in comparison with the adsorption energies, and due to some limitations of the solvation model for describing adsorption [54], the effects of implicit solvation have not been included in this work.

3. Results and discussion

3.1. Dry and wet CuO(111) and Cu(110)

The bare wet surfaces of CuO and Cu were prepared for the study of adsorption of the glucoside monomers by the subsequent creation of 1 ML of adsorbed H_2O on the initially dry surfaces, generating structures similar to those reported in previous works [30,37–39]. The difference between the current case and the cited works is that significantly larger supercells are here employed. The perfect Cu(110) surface can be used to simulate molecular adsorption onto real Cu surfaces with good accuracy because it contains 5 symmetrically non-equivalent binding sites [38]. These different coordination sites can to a good extent mimic the role of some point defects in molecular adsorption [39,55]. At the CuO(111) surface, point defects at room temperature have a smaller role in molecular adsorption because of the ionic nature of the bonding at the surface and its ease in relaxing, reconstructing and annihilating some of the defects [56].

Upon exposure of the dry surfaces to ambient air containing considerable moisture it is likely that additional MLs of H_2O form. However, the H_2O molecules at MLs far from the surface are not as relevant for the adsorption of the glucosides as the first ML of H_2O—the closest to the surfaces. This is because the bonds between H_2O and the surfaces are considerably stronger for the first ML and the H_2O in higher MLs are bound via H-bonds with similar strengths to those in liquid water [37]. The dry and wet surfaces are shown in Fig. 1. For Cu(110), the first ML of adsorbed water consists of alternating HO and H_2O along both directions A and B according to a previously reported structure [37]. For CuO(111), the surface here considered is fully covered with water, 1 ML, where the bound H_2O forms a pattern containing ½ ML of HO and ½ ML of H_2O [30], According to previous studies, in the lowest energy structure, these adsorbates are disposed in alternating rows of HO and H_2O, along the B direction. This was also observed in this study

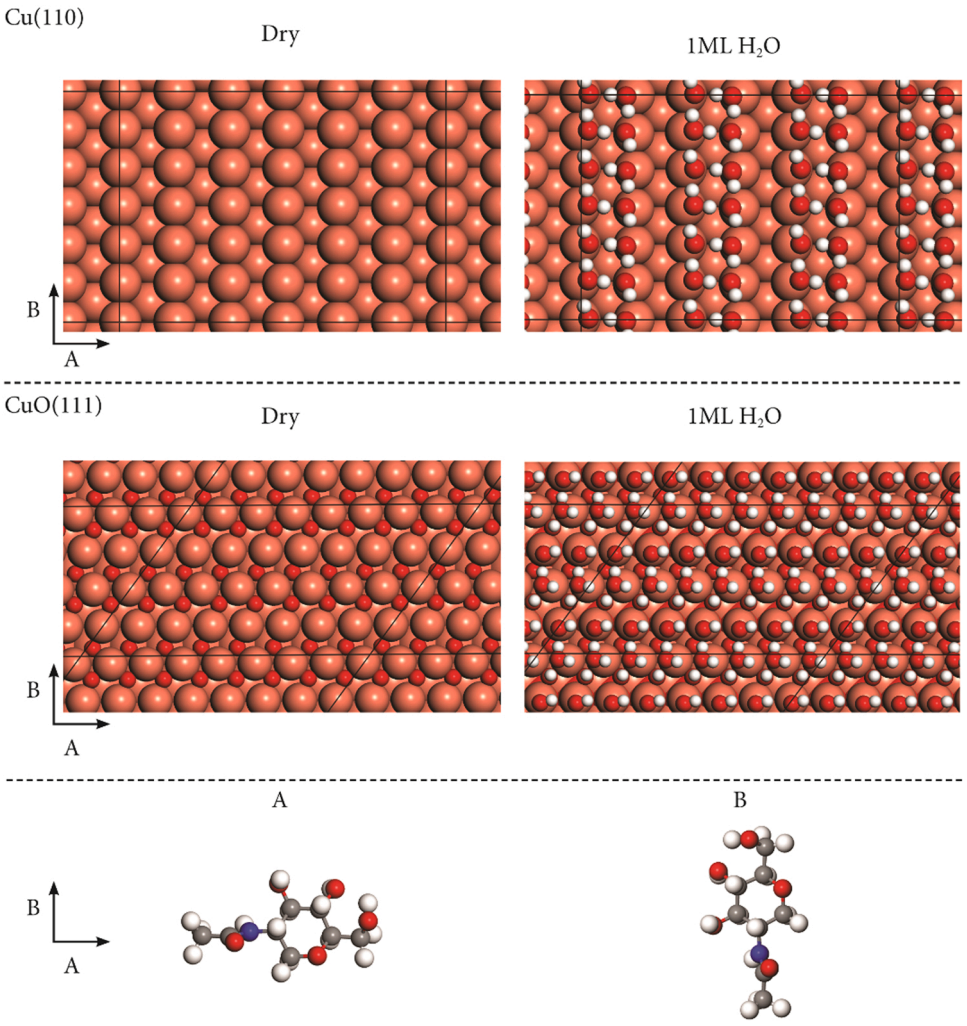

Fig. 1. Dry and wet surfaces of Cu(110) and CuO(111) employed in the study of the adsorption of the glucoside monomers. The axes A and B correspond to the following directions: A = [001], B = [$\bar{1}$10] in Cu(110); and A = [001], B = [011], in CuO(111). The black lines show the supercells. The bottom figures show the alignments of a glucoside relative to the axes A and B of the surfaces. These two alignments are designated by A and B, respectively. Cu (●), O (●), H (○).

and can be seen in Fig. 1.

The ΔE_{ads} values obtained for the molecular adsorption of 1 H_2O are in excellent agreement with previously published data: ΔE_{ads} (CuO) = −0.24 eV for the hollow site and − 0.19 eV for the ridge; [24] ΔE_{ads} (Cu) = −0.25 eV [55], The values obtained for 1 ML are also in very good agreement with literature data [37].

3.2. The glucoside monomers 6VSB, 6VXX and 6X6P

The structures of the glucoside monomers 6VSB, 6VXX and 6X6P in gas-phase were optimized starting from the PDB data with subsequent hydrogenation according to the known coordination rules for carbohydrates [57,58], leading to neutral molecules with singlet spin. No considerable changes to the structures have occurred upon geometry optimization with PBE-D3 which shows the good accuracy of the method for the structural modeling of these molecules. The resulting structures are shown in Fig. 2.

3.3. Interactions of 6VSB, 6VXX and 6X6P with dry and wet CuO(111) and Cu(110)

The monomers shown in Fig. 2 were placed at the surfaces in different orientations with the glucosidic O-atom (double bonded) pointing up as shown in the right-hand side panels of Fig. 2 or flipped with this O-atom pointing down towards the surface. For simplicity, these two orientations will respectively be referred to U and D from onwards. Additionally, the adsorption geometries of the monomers are labeled A, or B depending on the alignment between the monomer and the surface axes upon adsorption as shown in Fig. 1. The resulting structures are shown in Figs. 3 and 4 for CuO and Figs. 5 and 6 for Cu. The corresponding adsorption energies are shown in Figs. 7 and 8.

Figs. 3–6 show that the bonding between the glucosides and the surfaces occurs in two ways: via O-atoms (the glucosidic O-atom and alcohol O-atoms); and via H-atoms. This shows, contrary to what has been previously speculated, that van der Waals interactions play an important role in the adhesion of the virus to surfaces [59,60]. It is now widely known that van der Waals forces are present in both of these types of interactions with the surfaces, bonding via O and H-atoms, but it is more significant in the formation of H-bonds with the surfaces as previously shown for similar systems [37,61,62].

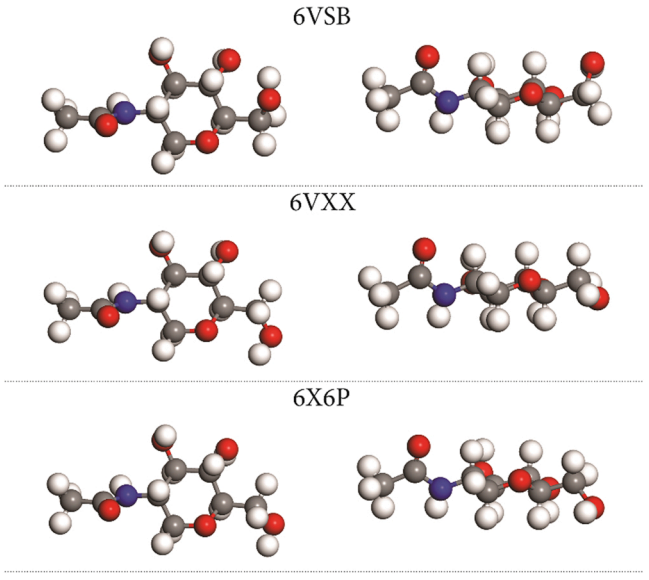

Fig. 2. Top and side views of the optimized structures of the glucoside monomers in gas-phase with PDB IDs: 6VSB, 6VXX and 6X6P; isomers of 2-acetamido-2-deoxy-beta-D-glucopyranose. C (●), O (●), N (●) H (○). The conformation 6VSB is β while 6VXX and 6X6P are α.

Due to its symmetry, the monomer 6VSB has both the glucosidic O-atom and the terminal alcohol O-atom pointing either towards the surface or away from it as shown in Fig. 2. While for the other two monomers either the glucosidic O-atom or the terminal alcohol O-atom point towards the surface. This leads to a larger dipole moment for 6VSB that affects both its ΔE_{ads} and adsorption geometry to very large extents. The result is that for the same surface, the ΔE_{ads} of 6VSB are considerably larger for all surfaces than for the other two monomers as shown in the data of Figs. 7 and 8. The exception to this is the wet Cu(110). A similar phenomenon has been previously observed for other adsorbates [38]. The increase in ΔE_{ads} happens because adsorbates with larger dipole moments induce also larger dipoles at the surface binding site and this increases their binding energy. Figs. 7 and 8 show also that the effect of the larger dipole in the adsorption energies of 6VSB is more pronounced for the dry surfaces. This is also in agreement with previous finds for other adsorbates. It is known that O-atoms bind stronger to Cu surfaces than H-atoms. This is also observed here for the studied monomers and causes a large dispersion in their adsorption energies which depend on if the monomers are oriented so that their glucosidic O-atoms point towards or away the surfaces. The adsorption structures show that for the conformations that lead to strong interactions with the surfaces, the bonds with the monomers are of a magnitude that causes the outwards dislocation of Cu atoms, a typical phenomenon that accompanies the formation of strong bonds with surfaces. This type of relaxation has been previously observed in the study of adsorption of H_2O onto this Cu surface [37]. At the dry Cu(110), the Cu-atoms that bind directly with the glucosidic O-atoms of the fragments expand outwards and their bond distances with the second layer of Cu-atoms changes by as much as 11% when compared to their equilibrium positions. The Cu-atoms that bind with the H-atoms of the fragments expand their bond distances with the second layer of Cu-atoms by only 0.5%, and those that bind via dispersion forces with the alcohol O-atom of the fragments expand by 1.8%. On average the expansions induced by the fragments when the glucosidic O-atom is pointing towards the surface is 6.4% and when the glucosidic O-atom points away from the surface is 1.6%. These different relaxations are the result of different chemical bonds: the covalent type bonding with the glucosidic O-atom; and the bonding with H-atoms and the OH group due to dispersion forces. For the cases where strong bonds occur the monomers also suffer considerable structural changes that affect internal bond lengths and angles.

The adsorption data shows that both Cu(110) and CuO(111) bind the monomers stronger when the surfaces are dry, and also that for the same surface there are large differences in ΔE_{ads} depending on if the surface is dry or wet. This effect is especially evident for metallic Cu. As visible in Figs. 3–6, the reason for this is that the chemical environment of the surface changes drastically from dry to wet Cu(110), while the difference between dry and wet CuO(111) is smaller because the dry CuO (111) is also composed of O-atoms. The latter case leads to similar bonds between the monomers and either dry CuO(111) or wet CuO(111), while for Cu(110) the monomers bind via very different types of bonds depending if the surface is dry or wet. For the dry surfaces, the larger standard deviations for ΔE_{ads} shown in the set of data of Fig. 8 highlight the fact that the bonding between the monomers and these surfaces is more sensitive to the orientation and conformation of the monomers. This is also expected according to previous finds for other molecules [37] because the bonding between the monomers and the dry surfaces has a higher dependency on the surface sites—top, long bridge, short bridge, etc—while for wet surfaces the bonding occurs via H-bonds with O-atoms. This type of environment is more flexible in terms of orientation of adsorbates and has more local minima in what concerns stable binding sites than for the case of dry surfaces.

Figs. 7 and 8 show that between the orientation of the monomers (U or D) and their alignment (A or B), the orientation is the factor that has the largest effect on ΔE_{ads}. Again the dry surfaces are those where the orientation U or D has a larger effect on ΔE_{ads} with differences that can

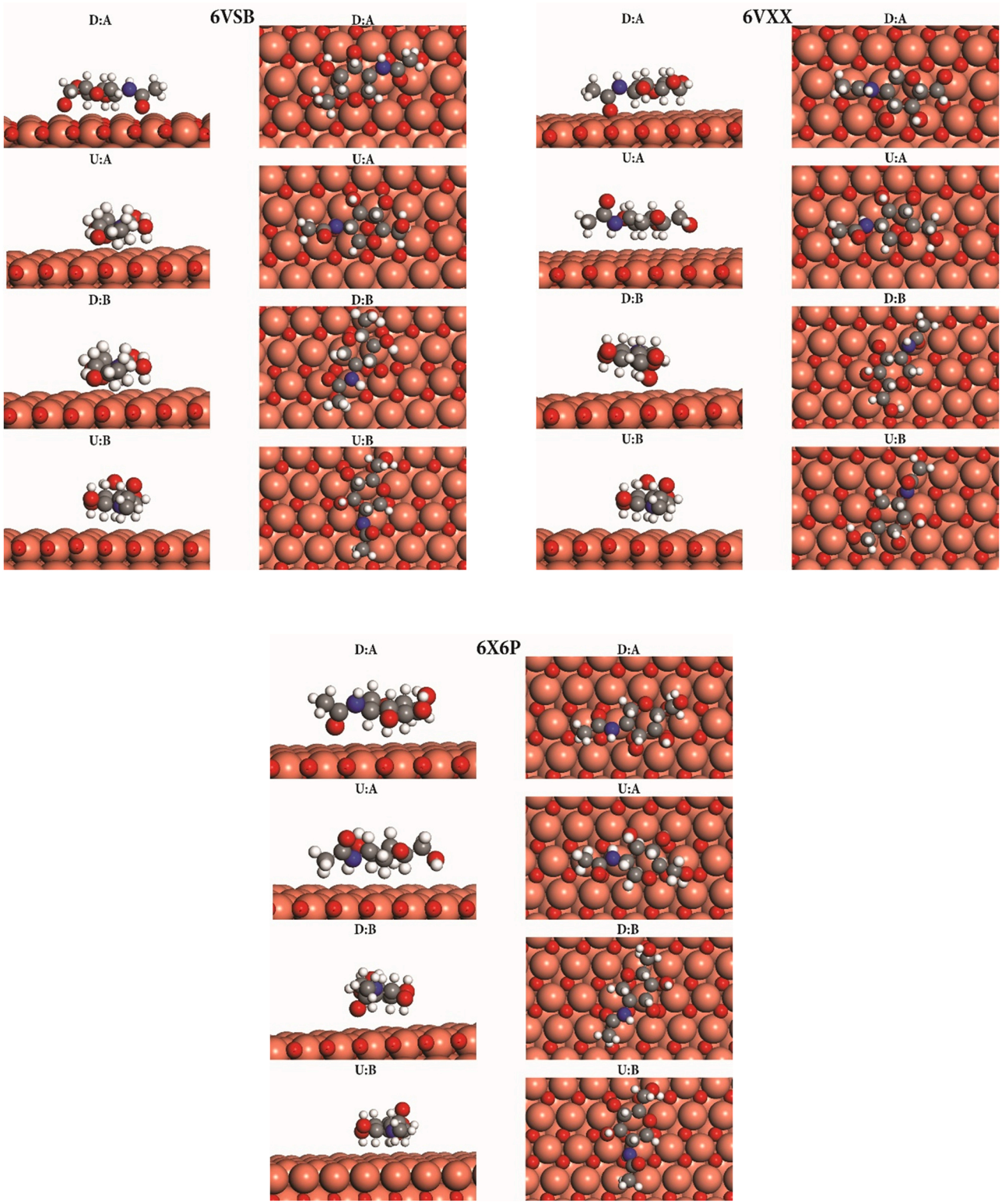

Fig. 3. Adsorption geometries for the monomers 6VSB, 6VXX and 6X6P at dry CuO(111). The monomers are oriented as U or D and A or B (see beginning of Section 3.3 for explanation).

Fig. 4. Adsorption geometries for the monomers 6VSB, 6VXX and 6X6P at wet CuO(111). The monomers are oriented as U or D and A or B (see beginning of Section 3.3 for explanation).

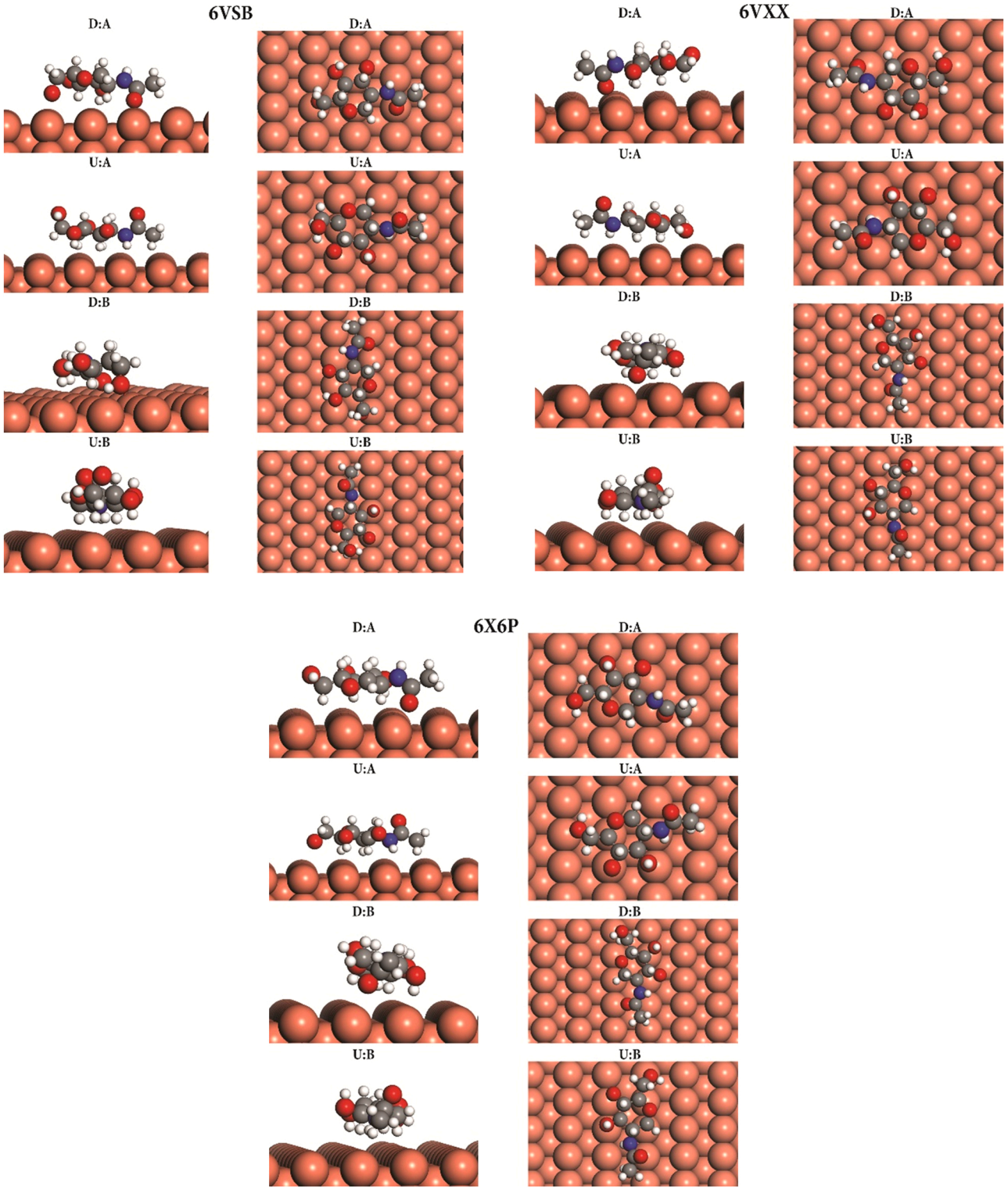

Fig. 5. Adsorption geometries for the monomers 6VSB, 6VXX and 6X6P at dry Cu(110). The monomers are oriented as U or D and A or B (see beginning of Section 3.3 for explanation).

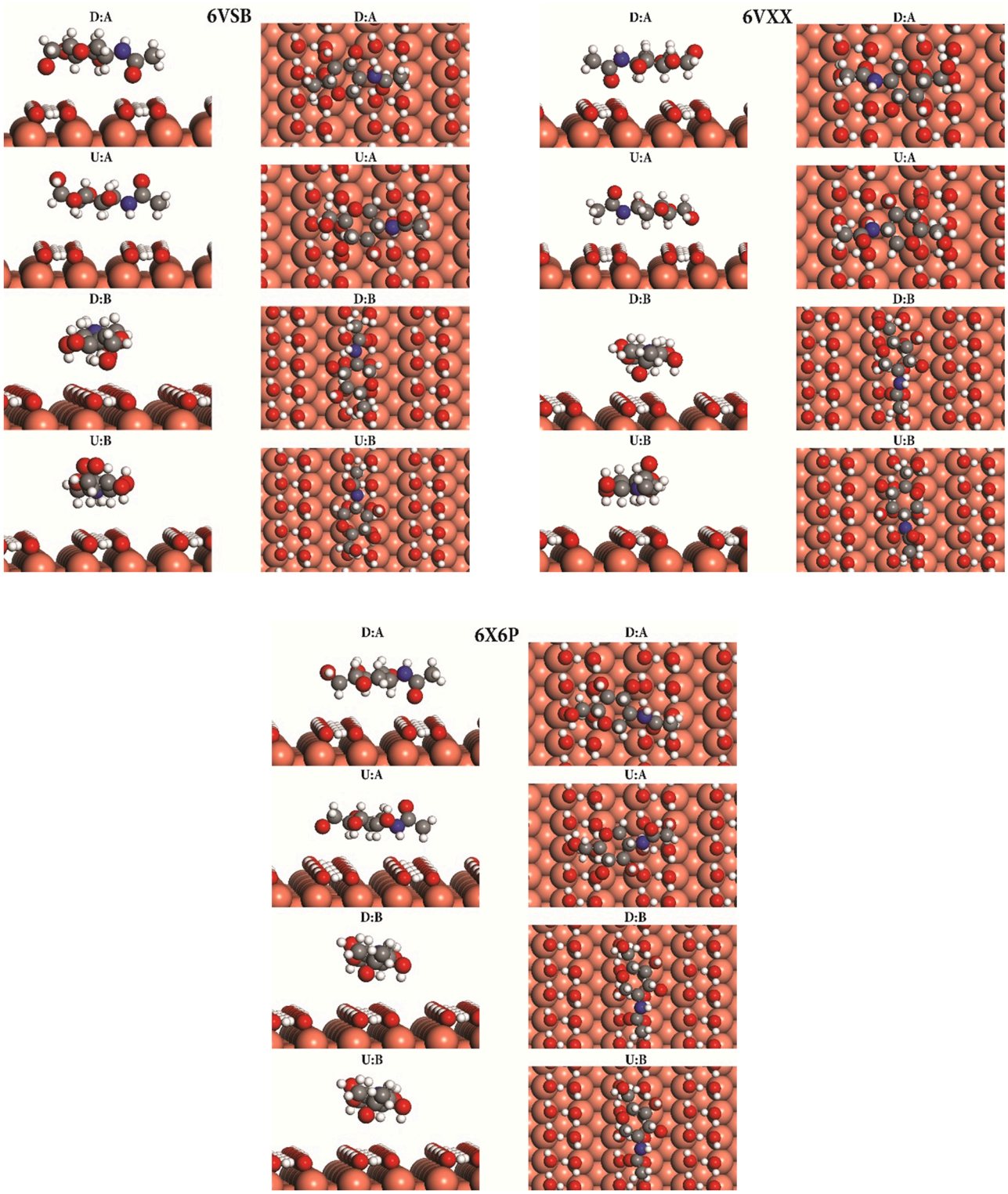

Fig. 6. Adsorption geometries for the monomers 6VSB, 6VXX and 6X6P at wet Cu(110). The monomers are oriented as U or D and A or B (see beginning of Section 3.3 for explanation).

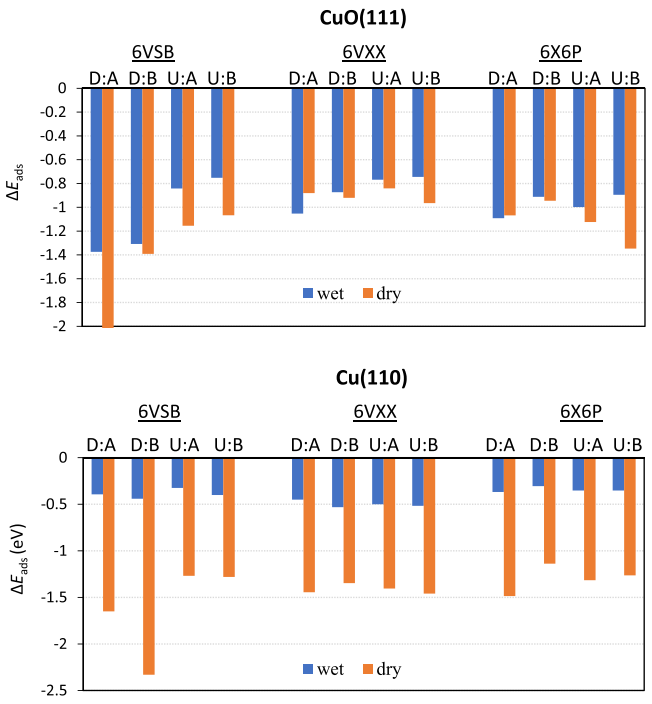

Fig. 7. Adsorption energies for the monomers 6VSB, 6VXX and 6X6P at dry and wet surfaces of CuO(111) and Cu(110). The monomers are oriented as U or D and A or B (see beginning of Section 3.3 for explanation).

reach 1 eV. The stronger bonds to the dry surfaces are of the order of − 2.2 eV for some cases. This is in agreement with previous observations that show that the virus can stick to Cu surfaces with considerably large forces per unit surface area [12]. The bonds here observed are very strong considering that these are molecular adsorption energies and do not involve bond breaking in the monomers at this point. Such strong bonds—which are almost 10 times stronger than H-bonds in water—can cause the tip of the S1 protein to be immobile as previously found for other proteins [63]. For the cases where the monomers bind very strongly to the surfaces, the complex "monomer-surface binding site" is subject to considerable structural changes as seen in Fig. 3–6. The stronger interactions between the monomers and the surfaces are expected to be able to drive the restructuring of the spike protein as it has been previously observed for a β-lactamase inhibitor protein when binding to a gold surface and for a lysozyme interacting with a SiO_2 surface [63,64]. In the first work cited, interactions of ≈ 0.6 to ≈ 1 eV were able to trigger the restructuring of the protein leading to loss of function. In the current case it is expected that some of the large binding energies with the surfaces will also lead to similar effects. This can have repercussions on the structure of the virus adjacent to the monomers of the tip of S1 and will consequently have effects in subsequent sections of the tip of spike protein directly connected to these sections. This could explain the shorter survival times of the virus at dry surfaces when compared to wet surfaces [10]. These results agree also with previous observations that show that the solvation of the interface between surfaces and the virus are the most important parameter that determine the life-time of the virus at these surfaces as well as the transmission rate of viral particles between surfaces [53]. Overall, the adsorption energies of Fig. 8 show that the interactions between the monomers and the dry surfaces are much stronger than for the wet surfaces, especially for Cu (110). The difference between the ΔE_{ads} of the monomers onto both the dry and the wet surfaces is larger than ΔE_{ads} of H_2O to these surfaces and also larger than the typical solvation energies of sugar monomers [65,66]. This implies that energetically, the adsorption of the monomers to the wet surfaces could cause the desorption of H_2O which would lead to direct bonds between the monomers and the surfaces—without the presence of interfacial H_2O at the contact point between the monomer and the surface. This would cause much stronger interactions between the monomers and the surfaces as shown in Fig. 8, which could trigger the inactivation mechanism. In this sense the mechanism of viral inactivation could occur even in the presence of water but would be slowed down due to kinetics and not because it is energetically unfavorable. However, real life studies are necessary to confirm the statistical occurrence of these phenomena because as the complete sets of adsorption data and the standard deviations show, there are many local minima in terms of stable binding sites for the glucosides to form bonds with the surfaces.

4. Conclusions

The interactions between glucoside monomers of the tip of the S1 subunit of SARS-CoV-2 spike protein and dry and wet surfaces of CuO and Cu were here studied with dispersion corrected DFT calculations. The three glucoside monomers that constitute the tip of the S1 subunit: 6VSB, 6VXX and 6X6P, were disposed at the dry and wet surfaces with different orientations and alignments. The very large differences in binding energies (adsorption energies) between these monomers and the surfaces are attributed to the type of surface, the presence of water, and to the orientation of the monomer—if the glucosidic O-atom points towards or away from the surfaces. Due to a larger dipole moment, the monomer 6VSB has considerably larger adsorption energies that can reach − 2.2 eV, but all three monomers bind to the surfaces with very large binding energies considering that the process is the molecular adsorption and does not involve bond breaking in the monomers at this stage. For the cases where the bonds with the surfaces are very strong the monomers are subject to considerable structural changes and in the case of Cu(110), the surface sites that bind to the glucosidic O-atom of the monomers are subject to considerable outward relaxation. Both materials bind the monomers present at the tip of the S1 group of the spike protein more strongly in dry conditions. For Cu(110), the whole set of data shows that the monomers bind to this surface on average 1 eV stronger when the surface is dry when compared to wet. The difference between dry and wet CuO(111) is smaller, in the order of 0.2 eV. The adsorption energies of H_2O onto these surfaces and the typical solvation energies of such sugar monomers suggest that the stronger bonds between the monomers and the dry surfaces can be enough to displace water molecules from the interface and create direct contacts between the monomers and the surfaces. However, this process can be hindered by kinetic constraints.

Overall these results show that the stability of the different monomers present in tip of the spike protein of the virus is very different at different surfaces and these differences depend largely on if the surfaces are wet or dry. The very large binding energies between the glucoside monomers and the dry surfaces and the structural changes that the monomers suffer in those cases can possibly lead to restructuring of the spike protein and its loss of function as previously observed for other proteins.

CRediT authorship contribution statement

Cláudio M. Lousada: Conceptualized the work, performed the investigation and wrote the paper.

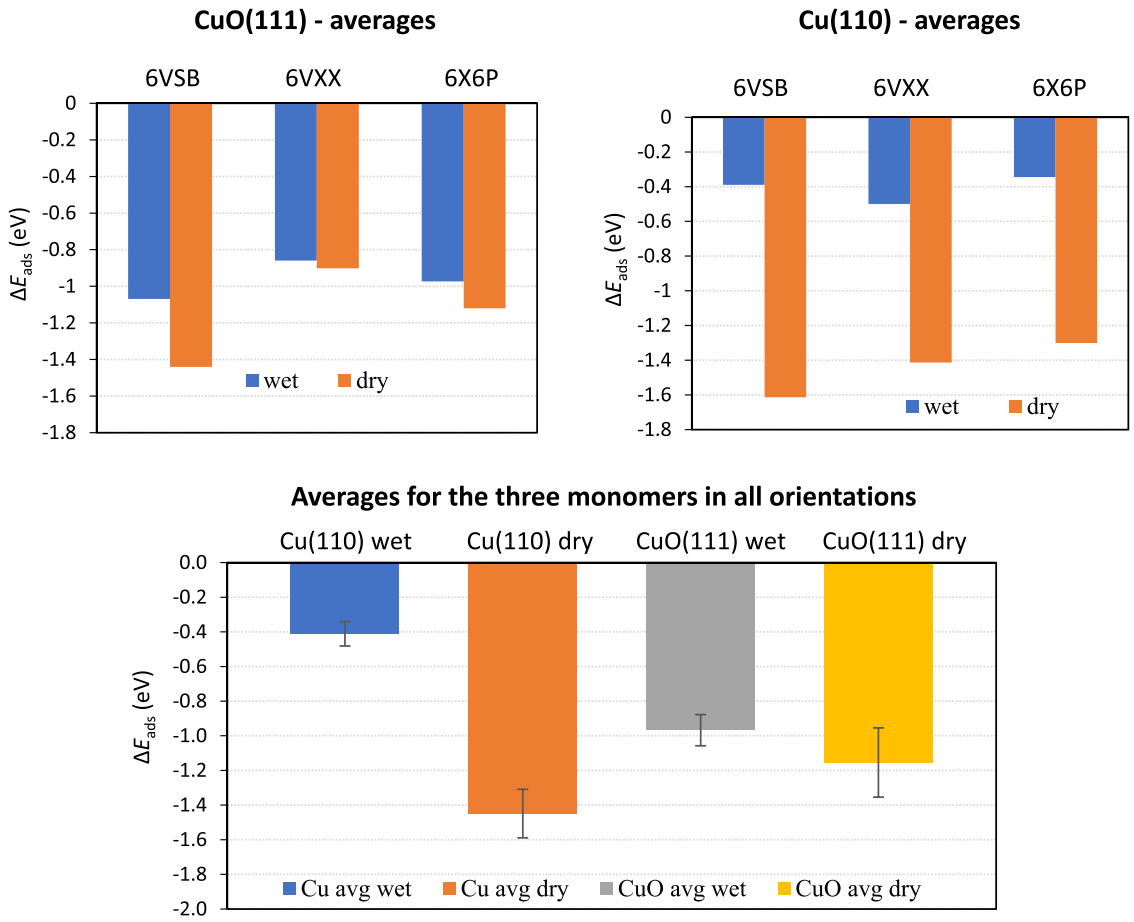

Fig. 8. Adsorption energies (ΔE_{ads}) for the monomers 6VSB, 6VXX and 6X6P at dry and wet surfaces of CuO(111) and Cu(110). Upper panels: average adsorption energies for each of the monomers obtained from the different orientations U or D and alignments A or B (see beginning of Section 3.3 for explanation). Lower panel: average adsorption energies for the three monomers in all conformations at each of the surfaces. The bars in the bottom figure are the standard deviations and represent the dispersion in the binding energies which in turn depend on the diversity of binding sites at the respective surface.

Declaration of Competing Interest

The authors declare that they have no known competing financial interests or personal relationships that could have appeared to influence the work reported in this paper.

Acknowledgements

The computations were performed on resources provided by the Swedish National Infrastructure for Computing (SNIC) at the High-Performance Computing Center North (HPC2N), Umeå and at the PDC Center for High Performance Computing at the KTH - Royal Institute of Technology, Stockholm, partially funded by the Swedish Research Council through grant agreement no. 2018-05973. Åke Sandgren at HPC2N is gratefully acknowledged for technical support. Pavel A. Korzhavyi and Rolf Sandström (Department of Materials Science and Engineering, Royal Institute of Technology - KTH, Stockholm, Sweden) are gratefully acknowledged for their help with access to computational tools necessary to perform this work.

References

[1] G. Kampf, D. Todt, S. Pfaender, E. Steinmann, Persistence of coronaviruses on inanimate surfaces and their inactivation with biocidal agents, J. Hosp. Infect. 104 (2020) 246–251.
[2] N. van Doremalen, T. Bushmaker, D.H. Morris, M.G. Holbrook, A. Gamble, B. N. Williamson, A. Tamin, J.L. Harcourt, N.J. Thornburg, S.I. Gerber, J.O. Lloyd-Smith, E. de Wit, V.J. Munster, Aerosol and Surface Stability of SARS-CoV-2 as Compared with SARS-CoV-1, New Engl. J. Med. 382 (2020) 1564–1567.
[3] M.U., Mondelli M., Colaneri E.M., Seminari F., Baldanti R. Bruno Low risk of SARS-CoV-2 transmission by fomites in real-life conditions. The Lancet Infectious Diseases.
[4] A.C. Luntz, in: A. Nilsson, et al. (Eds.), Chemical Bonding at Surfaces and Interfaces, Elsevier, Amsterdam, 2008, pp. 143–254.
[5] A. Nilsson, L.G.M. Pettersson, in: A. Nilsson, et al. (Eds.), Chemical Bonding at Surfaces and Interfaces, Elsevier, Amsterdam, 2008, pp. 57–142.
[6] D.P. Woodruff, in: A. Nilsson, et al. (Eds.), Chemical Bonding at Surfaces and Interfaces, Elsevier, Amsterdam, 2008, pp. 1–56.
[7] W. Mönch, Semiconductor Surfaces and Interfaces, Springer Berlin Heidelberg, Berlin, Heidelberg, 2001, pp. 377–384.
[8] A.L. Sumner, E.J. Menke, Y. Dubowski, J.T. Newberg, R.M. Penner, J. C. Hemminger, L.M. Wingen, T. Brauers, B.J. Finlayson-Pitts, The nature of water on surfaces of laboratory systems and implications for heterogeneous chemistry in the troposphere, Phys. Chem. Chem. Phys. 6 (2004) 604–613.
[9] A.W.H. Chin, J.T.S. Chu, M.R.A. Perera, K.P.Y. Hui, H.-L. Yen, M.C.W. Chan, M. Peiris, L.L.M. Poon, Stability of SARS-CoV-2 in different environmental conditions, Lancet Microbe 1 (2020), e10.
[10] R. Bhardwaj, A. Agrawal, How coronavirus survives for days on surfaces, Phys. Fluids 32 (2020), 111706.
[11] S. Bangaru, G. Ozorowski, H.L. Turner, A. Antanasijevic, D. Huang, X. Wang, J. L. Torres, J.K. Diedrich, J.-H. Tian, A.D. Portnoff, N. Patel, M.J. Massare, J. R. Yates, D. Nemazee, J.C. Paulson, G. Glenn, G. Smith, A.B. Ward, Structural analysis of full-length SARS-CoV-2 spike protein from an advanced vaccine candidate, Science 370 (2020) 1089–1094.
[12] L. Xie, F. Liu, J. Liu, H. Zeng, A nanomechanical study on deciphering the stickiness of SARS-CoV-2 on inanimate surfaces, ACS Appl. Mater. Interfaces 12 (2020) 58360–58368.
[13] F.R. Rehak, G. Piccini, M. Alessio, J. Sauer, Including dispersion in density functional theory for adsorption on flat oxide surfaces, in metal–organic frameworks and in acidic zeolites, Phys. Chem. Chem. Phys. 22 (2020) 7577–7585.
[14] Y. Jiang, S. Yang, S. Li, W. Liu, Aromatic molecules on low-index coinage metal surfaces: many-body dispersion effects, Sci. Rep. 6 (2016) 39529.
[15] Y. Huang, C. Yang, X.-f Xu, W. Xu, S.-w Liu, Structural and functional properties of SARS-CoV-2 spike protein: potential antivirus drug development for COVID-19, Acta Pharmacol. Sin. 41 (2020) 1141–1149.

[16] E.M. Rhea, A.F. Logsdon, K.M. Hansen, L.M. Williams, M.J. Reed, K.K. Baumann, S. J. Holden, J. Raber, W.A. Banks, M.A. Erickson, The S1 protein of SARS-CoV-2 crosses the blood–brain barrier in mice, Nat. Neurosci. (2020).
[17] J.K. Millet, G.R. Whittaker, Physiological and molecular triggers for SARS-CoV membrane fusion and entry into host cells, Virology 517 (2018) 3–8.
[18] Z. Hu, J.-P. Chen, J.-C. Xu, Z.-Y. Chen, R. Qu, L. Zhang, W. Yao, J. Wu, H. Yang, D. B. Lowrie, Y. Liu, X.-Y. Fan, A two-dose optimum for recombinant S1 protein-based COVID-19 vaccination, Virology 566 (2022) 56–59.
[19] F.X. Heinz, K. Stiasny, Distinguishing features of current COVID-19 vaccines: knowns and unknowns of antigen presentation and modes of action, npj Vaccin. 6 (2021) 104.
[20] N. S.N, R. B.N, P. C, S. K.S, T. Ramakrishnappa, K. B.T, J. S.M, M. M, A. N, D.D. P. Yallappa, R. T.V, G. E, M. Bagoji, S.S. Chandaragi, SARS-CoV 2 spike protein S1 subunit as an ideal target for stable vaccines: a bioinformatic study, Mater. Today: Proc. 49 (2022) 904–912.
[21] D. Wrapp, N. Wang, K.S. Corbett, J.A. Goldsmith, C.-L. Hsieh, O. Abiona, B. S. Graham, J.S. McLellan, Cryo-EM structure of the 2019-nCoV spike in the prefusion conformation, Science 367 (2020) 1260–1263.
[22] A.C. Walls, Y.-J. Park, M.A. Tortorici, A. Wall, A.T. McGuire, D. Veesler, Structure, function, and antigenicity of the SARS-CoV-2 spike glycoprotein, Cell 181 (2020) 281–292. .e6.
[23] N.G. Herrera, N.C. Morano, A. Celikgil, G.I. Georgiev, R.J. Malonis, J.H. Lee, K. Tong, O. Vergnolle, A.B. Massimi, L.Y. Yen, A.J. Noble, M. Kopylov, J. B. Bonanno, S.C. Garrett-Thomson, D.B. Hayes, R.H. Bortz, A.S. Wirchnianski, C. Florez, E. Laudermilch, D. Haslwanter, J.M. Fels, M.E. Dieterle, R.K. Jangra, J. Barnhill, A. Mengotto, D. Kimmel, J.P. Daily, L.-a Pirofski, K. Chandran, M. Brenowitz, S.J. Garforth, E.T. Eng, J.R. Lai, S.C. Almo, Characterization of the SARS-CoV-2 S protein: biophysical, biochemical, structural, and antigenic analysis, bioRxiv 2020 (2020), 06.14.150607.
[24] N.N. Greenwood, A. Earnshaw, in: N.N. Greenwood, A. Earnshaw (Eds.), Chemistry of the Elements, Second ed., Butterworth-Heinemann, Oxford, 1997, pp. 1173–1200.
[25] W. Steurer, in: K.H.J. Buschow, et al. (Eds.), Encyclopedia of Materials: Science and Technology, Elsevier, Oxford, 2001, pp. 1880–1897.
[26] H. Rieley, G.K. Kendall, R.G. Jones, D.P. Woodruff, X-ray studies of self-assembled monolayers on coinage metals. 2. Surface adsorption structures in 1-octanethiol on Cu(111) and Ag(111) and their determination by the normal incidence X-ray standing wave technique, Langmuir 15 (1999) 8856–8866.
[27] R. Caputo, B.P. Prascher, V. Staemmler, P.S. Bagus, C. Wöll, Adsorption of benzene on coinage metals: a theoretical analysis using wavefunction-based methods, J. Phys. Chem. A 111 (2007) 12778–12784.
[28] I. Platzman, R. Brener, H. Haick, R. Tannenbaum, Oxidation of polycrystalline copper thin films at ambient conditions, J. Phys. Chem. C 112 (2008) 1101–1108.
[29] A.K. Mishra, A. Roldan, N.H. de Leeuw, CuO surfaces and CO_2 activation: a dispersion-corrected DFT+U study, J. Phys. Chem. C 120 (2016) 2198–2214.
[30] M. Fronzi, M. Nolan, First-principles analysis of the stability of water on oxidised and reduced CuO(111) surfaces, RSC Adv. 7 (2017) 56721–56731.
[31] J. Zhang, R. Zhang, B. Wang, L. Ling, Insight into the adsorption and dissociation of water over different CuO(111) surfaces: The effect of surface structures, Appl. Surf. Sci. 364 (2016) 758–768.
[32] J.K. Nørskov, T. Bligaard, J. Rossmeisl, C.H. Christensen, Towards the computational design of solid catalysts, Nat. Chem. 1 (2009) 37–46.
[33] J.K. Nørskov, F. Abild-Pedersen, F. Studt, T. Bligaard, Density functional theory in surface chemistry and catalysis, Proc. Natl. Acad. Sci. USA 108 (2011) 937–943.
[34] M. Mavrikakis, A search engine for catalysts, Nat. Mater. 5 (2006) 847–848.
[35] J. Greeley, T.F. Jaramillo, J. Bonde, I. Chorkendorff, J.K. Nørskov, Computational high-throughput screening of electrocatalytic materials for hydrogen evolution, Nat. Mater. 5 (2006) 909–913.
[36] P. Sautet, F. Delbecq, Catalysis and surface organometallic chemistry: a view from theory and simulations, Chem. Rev. 110 (2010) 1788–1806.
[37] C.M. Lousada, A.J. Johansson, P.A. Korzhavyi, Thermodynamics of H_2O Splitting and H_2 Formation at the Cu(110)–Water Interface, J. Phys. Chem. C 119 (2015) 14102–14113.
[38] C.M. Lousada, A.J. Johansson, P.A. Korzhavyi, Adsorption of hydrogen sulfide, hydrosulfide and sulfide at Cu(110) - polarizability and cooperativity effects. first stages of formation of a sulfide layer, ChemPhysChem 19 (2018) 2159–2168.
[39] C.M. Lousada, A.J. Johansson, P.A. Korzhavyi, Molecular and dissociative adsorption of water and hydrogen sulfide at perfect and defective Cu(110) surfaces, Phys. Chem. Chem. Phys. 19 (2017) 8111–8120.
[40] G. Kresse, J. Furthmüller, Efficient iterative schemes for ab initio total-energy calculations using a plane-wave basis set, Phys. Rev. B 54 (1996) 11169–11186.
[41] J.P. Perdew, K. Burke, M. Ernzerhof, Generalized gradient approximation made simple, Phys. Rev. Lett. 77 (1996) 3865–3868.
[42] J.P. Perdew, K. Burke, M. Ernzerhof, Generalized gradient approximation made simple [Phys. Rev. Lett. 77, 3865 (1996)], Phys. Rev. Lett. 78 (1997) 1396 (-).
[43] P.E. Blöchl, Projector augmented-wave method, Phys. Rev. B 50 (1994) 17953–17979.
[44] G. Kresse, D. Joubert, From ultrasoft pseudopotentials to the projector augmented-wave method, Phys. Rev. B 59 (1999) 1758–1775.
[45] C.M. Lousada, Wood cellulose as a hydrogen storage material, Int. J. Hydrogen Energy 45 (2020) 14907–14914.
[46] J. Moellmann, S. Grimme, DFT-D3 study of some molecular crystals, J. Phys. Chem. C 118 (2014) 7615–7621.
[47] C.M. Lousada, N. Sophonrat, W. Yang, Mechanisms of formation of H, HO, and water and of water desorption in the early stages of cellulose pyrolysis, J. Phys. Chem. C 122 (2018) 12168–12176.
[48] S. Grimme, J. Antony, S. Ehrlich, H. Krieg, A consistent and accurate ab initio parametrization of density functional dispersion correction (DFT-D) for the 94 elements H-Pu, J. Chem. Phys. 132 (2010), 154104.
[49] H.J. Monkhorst, J.D. Pack, Special points for Brillouin-zone integrations, Phys. Rev. B 13 (1976) 5188–5192.
[50] S. Asbrink, A. Waskowska, CuO: X-ray single-crystal structure determination at 196 K and room temperature, J. Phys.: Condens. Matter 3 (1991) 8173–8180.
[51] K. Mathew, R. Sundararaman, K. Letchworth-Weaver, T.A. Arias, R.G. Hennig, Implicit solvation model for density-functional study of nanocrystal surfaces and reaction pathways, J. Chem. Phys. 140 (2014), 084106.
[52] K. Mathew, V.S.C. Kolluru, S. Mula, S.N. Steinmann, R.G. Hennig, Implicit self-consistent electrolyte model in plane-wave density-functional theory, J. Chem. Phys. 151 (2019), 234101.
[53] W.C.K. Poon, A.T. Brown, S.O.L. Direito, D.J.M. Hodgson, L. Le Nagard, A. Lips, C. E. MacPhee, D. Marenduzzo, J.R. Royer, A.F. Silva, J.H.J. Thijssen, S. Titmuss, Soft matter science and the COVID-19 pandemic, Soft Matter 16 (2020) 8310–8324.
[54] Q. Zhang, A. Asthagiri, Solvation effects on DFT predictions of ORR activity on metal surfaces, Catal. Today 323 (2019) 35–43.
[55] C.M. Lousada, A.J. Johansson, P.A. Korzhavyi, Molecular and dissociative adsorption of water at a defective Cu(110) surface, Surf. Sci. 658 (2017) 1–8.
[56] L. Li, G. Chen, H. Zheng, W. Meng, S. Jia, L. Zhao, P. Zhao, Y. Zhang, S. Huang, T. Huang, J. Wang, Room-temperature oxygen vacancy migration induced reversible phase transformation during the anelastic deformation in CuO, Nat. Commun. 12 (2021) 3863.
[57] A.G. Gerbst, V.B. Krylov, N.E. Nifantiev, Carbohydrate Chemistry: Chemical and Biological Approaches, 44, The Royal Society of Chemistry, 2021, pp. 151–169.
[58] A. Arda, U. Atxabal, S. Bertuzzi, A. Canales, F.J. Cañada, A. Gimeno, J. Ereño-Orbea, B.F. de Toro, A. Franconetti, M. Gómez-Redondo, M.G. Lete, M.P. Lenza, J. D. Martínez, M.J. Moure, A. Poveda, J.I. Quintana, P. Valverde, J. Jiménez-Barbero, Carbohydrate Chemistry: Chemical and Biological Approaches, 44, The Royal Society of Chemistry, 2021, pp. 170–194.
[59] G.W. Fuhs, M. Chen, L.S. Sturman, R.S. Moore, Virus adsorption to mineral surfaces is reduced by microbial overgrowth and organic coatings, Microb. Ecol. 11 (1985) 25–39.
[60] M.O. Aydogdu, E. Altun, E. Chung, G. Ren, S. Homer-Vanniasinkam, B. Chen, M. Edirisinghe, Surface interactions and viability of coronaviruses, J. R. Soc. Interface 18 (2021), 20200798.
[61] J. Carrasco, J. Klimeš, A. Michaelides, The role of van der Waals forces in water adsorption on metals, J. Chem. Phys. 138 (2013), 024708.
[62] P.O. Bedolla, G. Feldbauer, M. Wolloch, S.J. Eder, N. Dörr, P. Mohn, J. Redinger, A. Vernes, Effects of van der Waals interactions in the adsorption of isooctane and ethanol on Fe(100) surfaces, J. Phys. Chem. C 118 (2014) 17608–17615.
[63] M. Ozboyaci, D.B. Kokh, R.C. Wade, Three steps to gold: mechanism of protein adsorption revealed by Brownian and molecular dynamics simulations, Phys. Chem. Chem. Phys. 18 (2016) 10191–10200.
[64] K. Kubiak-Ossowska, P.A. Mulheran, Multiprotein interactions during surface adsorption: a molecular dynamics study of lysozyme aggregation at a charged solid surface, J. Phys. Chem. B 115 (2011) 8891–8900.
[65] V. Spiwok, I. Tvaroška, Conformational free energy surface of α-N-acetylneuraminic acid: an interplay between hydrogen bonding and solvation, J. Phys. Chem. B 113 (2009) 9589–9594.
[66] Q. Du, D. Beglov, B. Roux, Solvation free energy of polar and nonpolar molecules in water: an extended interaction site integral equation theory in three dimensions, J. Phys. Chem. B 104 (2000) 796–805.